Robust Control of a Lightweight Structure for Digital Fabrication

Yvonne R. Stürz * **Andrea Iannelli** ** **Roy S. Smith** **

* *Model Predictive Control Laboratory, University of California, Berkeley, CA 94709, USA (e-mail: y.stuerz@berkeley.edu)*
** *Automatic Control Laboratory, ETH Zürich, ZH 8092, Switzerland (e-mail: {iannelli, rsmith}@control.ee.ethz.ch).*

Abstract: For a material efficient construction process of lightweight concrete shells, tensioned cable nets can be used as a supporting formwork. In order to guarantee the mechanical stability of the shells, tight tolerances in their form need to be met. To this end, methods have recently been proposed to readjust the form of the cable net on the construction site. This paper proposes a novel view on the cable net model as a dynamical system and derives robust control approaches based on $\mathcal{H}_\infty$ and μ synthesis. Both approaches can account for input uncertainties and external disturbances. The μ controller additionally is robust against the uncertain model parameters, which makes their precise identification unnecessary. The μ synthesis also provides a priori bounds on the allowable fabrication tolerances of the cable net in order to guarantee robust performance of the closed-loop system. The resulting LTI controllers can be applied to the system without expert knowledge about the system model or the underlying optimization. The effectiveness of the controllers is demonstrated in numerical experiments.

Keywords: Robust Control, Model Uncertainty, μ-Synthesis, Digital Fabrication, Lightweight Structures

1. INTRODUCTION

Doubly curved thin concrete shells are efficient building structures to span large areas (Torsing et al., 2012), as e.g. in roof applications. These shells can have a high structural stiffness while requiring less material, and therefore less energy than traditional building structures (Lydon et al., 2017). In the construction process of thin concrete shells, a supporting formwork, defining the form of the shell, is required. It is removed after the curing of the concrete. Traditional formwork, consisting of a huge number of customized parts, is time-, labor- and cost-intensive and produces a lot of waste. An alternative flexible formwork (Stürz et al., 2019) can be used instead. Its main component is a steel cable net which is prestressed inside a rigid frame. On top of the cable net, a fabric is placed, which builds the surface to support the concrete. This flexible formwork can reduce the amount of material used and waste produced compared to traditional formwork.

While fabrication tolerances for construction applications are not very tight in general, they are for the cable net geometry. The reason is that desired structural properties of the shell, such as mechanical stability and buckling behavior, can be guaranteed only within small variations from its desired target form. Achieving these allowable tolerances was shown to be impossible with traditional construction methods (Veenendaal et al., 2014). Therefore, feedback-based control methods have been introduced in order to adjust the cable net form and thus to minimize the deviations from the designed form during the construction process (Stürz et al., 2016a, 2019; Stürz, 2019). As measurements and actuation steps on the construction site are time-consuming and expensive, the number of their iterations should be minimized. To this end, model knowledge about the system is exploited in the control methods. The system model represents the static equilibria of the system. It involves a set of parameters which are subject to high fabrication variations and to which the cable net form is very sensitive. Therefore, the work in (Stürz et al., 2016b, 2020) has proposed methods for the identification of these uncertain system parameters. In (Stürz et al., 2019), the identification step is then combined with a control input computation (Stürz et al., 2016a) in an iterative algorithm to achieve a high precision control of the cable net form while minimizing the required measurement and actuation iterations. In (Stürz et al., 2019; Liew et al., 2018), these model- and optimization-based control methods are validated on a quarter-scale prototype of a roof shell. While a high precision is achieved, the control algorithm requires a lot of expert knowledge and its performance relies on the precision of the identified system parameters.

This paper addresses these recognized issues by exploiting techniques from robust control (Zhou et al., 1996). To this end, a novel modeling approach for the cable net is proposed by formulating it as a discrete-time linear time-invariant (LTI) dynamical system where at each time step a control input is applied. Exogenous disturbances (e.g. input uncertainties) and modeling uncertainties (e.g. fabrication variations) are then directly taken into account in the control design. Regulation and disturbance rejection problems are formulated within the $\mathcal{H}_\infty$ framework, whereas robustness of the closed loop to changes in the model parameters is achieved by μ synthesis, which also provides a bound on the allowed fabrication tolerances.

The paper is structured as follows. Section 2 provides a background to the robust control concepts employed in this work.

⋆ This project has received funding from the European Union's Horizon 2020 research and innovation programme under the Marie Sklodowska-Curie grant agreement No. 846421. This work was also partially supported by the Swiss National Science Foundation under grant no. 200021_178890.

In Section 3, a physical description of the cable net system and the mathematical definition of its static equilibrium is reviewed, before the problem formulation is stated. Section 4 derives a dynamical model, and Section 5 discusses the design of robust controllers via $\mathcal{H}_\infty$ and μ synthesis. Section 6 compares the performance of the controllers on a numerical example.

Notation: The identity matrix of dimension n and the matrices of all zeros and all ones of dimension $m \times n$ are denoted by I_n, $0_{m,n}$, and $1_{m,n}$, respectively. The Moore-Penrose pseudoinverse is denoted by $\dagger$, and the kronecker product by $\otimes$. We will use $M[q:p, r:s]$ to denote the block of the matrix M ranging over the rows q to p and over the columns r to s. The operator $\lceil\rangle\dashv\rfloor(v)$ maps the vector v to a matrix of all zeros zeros except the entries of v on its diagonal. For a function $f(x) : \mathbb{R}^n \mapsto \mathbb{R}$, we denote the gradient by $\nabla_x f = [\frac{\partial f}{\partial x_1} \ \cdots \ \frac{\partial f}{\partial x_n}]^\top$. For a function $h(r,u) : \mathbb{R}^{n+p} \mapsto \mathbb{R}^m$, the Jacobian is denoted by $\nabla_{(r,u)} h = [\nabla_r h \,|\, \nabla_u h]$, where $\nabla_{(r,u)}$ denotes the partial derivatives with respect to r and u, and $\nabla_r h$ and $\nabla_u h$ are referred to as partial Jacobians. We use $\nabla_{(r,u)} h(r^k, u^k)$ to denote the Jacobian evaluated at the point (r^k, u^k). The weighted L_2-norm with Q being a weighting matrix is denoted as $\|x\|_Q^2 = x^\top Q\, x$. Given a transfer matrix $G(s)$, its $\mathcal{H}_\infty$ norm is defined by $\|G\|_\infty = \sup_\omega \bar{\sigma}(G(j\omega))$, where $\bar{\sigma}(\cdot)$ denotes the maximum singular value of a matrix and ω denotes the frequency.

2. ROBUST CONTROL BACKGROUND

The Linear Fractional Transformation (LFT) is a fundamental tool in robust control to create models of uncertain systems suitable for analysis and synthesis (Zhou et al., 1996). Let $M \in \mathbb{C}^{(p_1+p_2)\times(q_1+q_2)}$ be a complex matrix partitioned as

$$M = \begin{bmatrix} M_{11} & M_{12} \\ M_{21} & M_{22} \end{bmatrix}, \tag{1}$$

and $\Delta_u \in \mathbb{C}^{q_1 \times p_1}$. The upper LFT of M w. r. t. Δ_u is given by

$$\mathcal{F}_u(M, \Delta_u) = M_{22} + M_{21}\Delta_u(I - M_{11}\Delta_u)^{-1} M_{12}. \tag{2}$$

An interpretation of (2) can be obtained by considering a nominal linear time invariant (LTI) system with transfer matrix M_{22} having input $v \in \mathbb{R}^{q_2}$ and output $y \in \mathbb{R}^{p_2}$ and subject to uncertainty modelled by an operator Δ_u. The transfer matrices M_{11}, M_{12} and M_{21} describe the effect of Δ_u on M_{22}, and $\mathcal{F}_u(M, \Delta_u)$ is the map between input and output of the plant in the presence of uncertainty, as shown in Fig. 1.

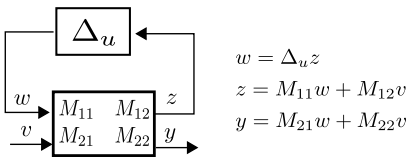

Fig. 1. Feedback representation of an LFT.

A crucial feature apparent in (2) is that the LFT is well posed, and thus the loop equations have a unique solution, if and only if the inverse of $(I - M_{11}\Delta_u)$ exists. Equivalently, the lower LFT of M w.r.t. $P_l \in \mathbb{C}^{q_2 \times p_2}$ is given by

$$\mathcal{F}_l(M, P_l) = M_{11} + M_{12} P_l (I - M_{22} P_l)^{-1} M_{21}. \tag{3}$$

One of the most celebrated design techniques from robust control is the $\mathcal{H}_\infty$ framework (Doyle and Stein, 1981), where performance is formulated in terms of the $\mathcal{H}_\infty$ norm of a certain transfer matrix. The search for such a controller K_∞ can be defined as the following optimization problem

$$\min_{K_\infty} \|\mathcal{F}_l(M, K_\infty)\|_\infty, \tag{4}$$

where $\mathcal{F}_l(M, K_\infty)$ is now the transfer matrix associated with the chosen performance objective. While $\mathcal{H}_\infty$ control makes the plant robust against *exogenous* disturbances, it does not address robustness against *endogenous* disturbances, such as for example parametric uncertainties in the model.

The μ analysis technique addresses robust stability and performance of LTI systems in the presence of *structured* uncertainty sets (Packard and Doyle, 1993). The uncertainty can be generically defined as $\Delta_u = \text{diag}(\delta_i I_{d_i}, \delta_j I_{d_j}, \Delta_{D_k})$, where the uncertainties associated with n_R real scalars, δ_i, n_C complex scalars, δ_j, and n_D unstructured (or full) complex blocks, Δ_{D_k}, are listed in diagonal form. The structured singular value (s.s.v.), denoted by $\mu_{\Delta_u}(M)$, is defined as

$$\mu_{\Delta_u}(M) = \left[\min_{\Delta_u} \Big(\kappa : \det(I - \kappa M \Delta_u) = 0;\ \bar{\sigma}(\Delta_u) \le 1\Big)\right]^{-1}, \tag{5}$$

where κ is a real positive scalar, and $\mu_{\Delta_u}(M) = 0$ if the minimization problem has no solution. If $\mu_{\Delta_u}(M) \le 1$ then the result guarantees that $\mathcal{F}_u(M, \Delta_u)$ is not ill-posed for uncertainties in the allowed set, hence the system is robustly stable. Conversely, if $\mu_\Delta(M) > 1$ the system can become unstable for particular combinations of the uncertainties, thus providing a worst-case robust stability (RS) test.

The s.s.v. can also be used for robust performance (RP) by considering the LFT $\mathcal{F}_u(M, \Delta)$, where $\Delta = \text{diag}(\Delta_u, \Delta_c)$ and the full-complex perturbation matrix Δ_c closes the loop between the input v and output y in Fig. 1. Building on the $\mathcal{H}_\infty$ synthesis and the μ analysis framework, the goal of μ synthesis is to find a controller K_μ which minimizes the maximum singular value of a certain closed loop transfer function in the face of the uncertainty Δ_u, that is

$$\begin{aligned} &\min_{K_\mu} \max_{\Delta_u} \|\mathcal{F}_u(\mathcal{F}_l(M, K_\mu), \Delta_u)\|_\infty, \\ \text{or equivalently} \quad &\min_{K_\mu} \mu_\Delta(\mathcal{F}_l(M, K_\mu)). \end{aligned} \tag{6}$$

The μ synthesis framework thus provides a controller which is robust to exogenous disturbances, because the objective is the minimization of the $\mathcal{H}_\infty$ norm, and uncertainties, since the $\mathcal{H}_\infty$ norm is taken over all the possible uncertainty realizations. A well established way to numerically solve (6) is the so-called D-K iteration (Packard et al., 1993), where one iterates between a μ calculation (D step) and an $\mathcal{H}_\infty$ design (K step). In this work the routine *dksyn* (Balas et al., 1998) currently available in the Robust Control Toolbox (RCT) will be used in MATLAB R2019b.

3. CABLE NET DESCRIPTION AND PROBLEM FORMULATION

In this section, we review the model of the cable net system and state the problem formulation.

3.1 Description of the Cable Net System

We consider the graph $\mathcal{G} = (\mathcal{N}, \mathcal{E})$ to encode the topology of the cable net. The node set $\mathcal{N}$ comprises the indices of the n nodes of the cable net, which are equipped with x-, y- and z-position coordinates. For each node, $i \in \mathcal{N}$, its position coordinates are stacked in the vector $r_i \in \mathbb{R}^3$. The edge set $\mathcal{E}$ represents the indices of the m cable segments of the net.

We refer to the nodes in the interior of the net as interior nodes and to the ones at the boundary on the rigid frame as boundary nodes. Similarly, the edges in the interior and at the boundary of the net are called interior and boundary edges, respectively. We will use the indices I and B to denote interior and boundary variables. The node and edge sets can be split into the two disjoint subsets of interior and boundary nodes or edges, respectively, i.e., $\mathcal{N} = \mathcal{N}_I \cup \mathcal{N}_B$, $\mathcal{N}_I \cap \mathcal{N}_B = \emptyset$, $\mathcal{E} = \mathcal{E}_I \cup \mathcal{E}_B$, $\mathcal{E}_I \cap \mathcal{E}_B = \emptyset$. In the following, we assume that the frame is rigid and does not bend or flex. Therefore, the positions of the boundary nodes, $r_i,\ i \in \mathcal{N}_B$, are assumed to be constant. The position coordinates of the interior nodes, $r_i,\ i \in \mathcal{N}_I$, define the form of the cable net. In the prestressed state, all cable net edges are in tension. In this state the edge lengths are the Euclidean distances between adjacent nodes. For the edge between nodes s and t, the edge length is given by

$$l_{(s,t)} := \|r_s - r_t\|_2. \tag{7}$$

We refer to *unstressed lengths* of the cable net edges as the lengths of the edges if no tension forces are acting on them. The vector of all unstressed edge lengths is denoted by

$$l_0 := [l_{0,1} \ \ ... \ \ l_{0,m}]^\top \in \mathbb{R}^m. \tag{8}$$

These unstressed cable net edge lengths are fixed parameters for all m_I interior edges. They are collected in the vector $l_{0,I} \in \mathbb{R}^{m_I}$. In contrast, the m_B boundary edges of the cable net are attached to the rigid frame via turnbuckles. Through actuation of the turnbuckles, the unstressed lengths of the boundary edges can be adjusted to change the form of the cable net. The parameters of unstressed lengths of the boundary edges are collected in the vector $l_{0,B} \in \mathbb{R}^{m_B}$. We define the input vector $u \in \mathbb{R}^{n_u}$, with $n_u = m_B$, as the vector collecting the adjustments to the unstressed boundary edge lengths, given by

$$u := [u_1\ ,\ ...\ ,\ u_{(s,t)}\ ,\ ...\ ,\ u_{m_B}]^\top \in \mathbb{R}^{m_B},\ \ \forall (s,t) \in \mathcal{E}_B, \tag{9}$$

where $u_{(s,t)}$ is the change in unstressed length $l_{0,(s,t)}$ for the boundary edge (s,t). We further define the unstressed length of edge (s,t) after actuation by the input $u_{(s,t)}$ as

$$\bar{l}_{0,(s,t)} = l_{0,(s,t)} - u_{(s,t)}\ ,\ \forall (s,t) \in \mathcal{E}_B. \tag{10}$$

Analogously, the notation $\bar{l}_{0,(s,t)} = l_{0,(s,t)}\ ,\ \forall (s,t) \in \mathcal{E}_I$ is also used in the case where (s,t) is a non-adjustable interior edge. Figure 2 shows a top view on the cable net system.

3.2 Force Balance Equations

We denote the mapping from the inputs u to the position coordinates r as $R(u)$, i.e.,

$$r = R(u). \tag{11}$$

This mapping is not explicitly known. Instead, the following mathematical characterization of the form of the cable net under the input u can be given. The static equilibrium of the cable net is characterized by a force balance of all the tension forces belonging to adjacent edges of the interior nodes. The set of adjacent edges of node s which are in tension is denoted by $\bar{\mathcal{E}}_s$.

The nodal position coordinates r in static equilibrium are therefore the solution to the following equations

$$\begin{aligned} h_s = &\sum_{(s,t)\in\bar{\mathcal{E}}_s} EA_{(s,t)}\,(r_s - r_t)\left(\frac{1}{\bar{l}_{0,(s,t)}} - \frac{1}{l_{(s,t)}}\right) - p \\ &= 0,\ \ \forall\ s \in \mathcal{N}_I, \end{aligned} \tag{12}$$

where $EA_{(s,t)}$ denotes the elastic material parameter of edge (s,t) and p is a vector of external forces acting on the nodes.

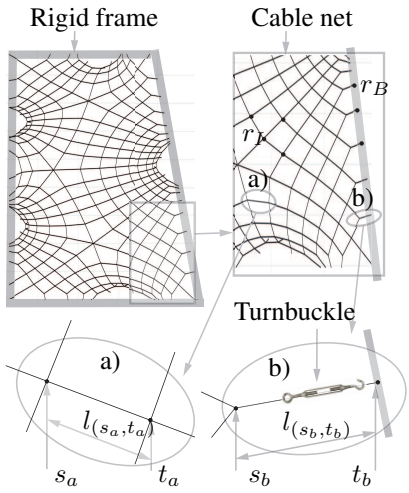

Fig. 2. Top view of the cable net system, (Stürz et al., 2019). a) Interior edge $(s_a, t_a) \in \mathcal{E}_I$ connecting the nodes $s_a \in \mathcal{N}_I$ and $t_a \in \mathcal{N}_I$. b) Boundary edge $(s_b, t_b) \in \mathcal{E}_B$ connecting the node $s \in \mathcal{N}_I$ and the node $t \in \mathcal{N}_B$. Control inputs are applied via the turnbuckle.

For fixed boundary coordinates, $r_B = \bar{r}_B$, the function $h : \mathbb{R}^{3n_I} \times \mathbb{R}^{m_B} \mapsto \mathbb{R}^{3n_I}$ represents all force equilibrium equations at all interior nodes, i.e.,

$$h(r_I, u) = \left[h_1^\top\ \ldots\ h_{n_I}^\top\right]^\top. \tag{13}$$

For more details about the modeling the static equilibrium of the cable net system, we refer to (Stürz et al., 2019).

3.3 Problem Formulation

The target form of the cable net, denoted by $r^{(\mathrm{des})}$, is given as the result of a design problem. The parameters l_0 are subject to high fabrication variations, and therefore to large uncertainties. In the construction of the prestressed cable net, the initial boundary edge lengths need to be set to their nominal values which is a manual process introducing large uncertainties.

The control problem consists of using the available control inputs in form of boundary edge lengths adjustments, u, in order to steer the cable net form, $r = R(u)$, as close as possible to the given desired form, $r^{(\mathrm{des})}$. The control approach should be robust w.r.t. the uncertainties in the model parameters, while also considering uncertainties in the control inputs and possible other disturbances on the net. A bound on the allowable fabrication tolerances on the unstressed cable net edge lengths $l_{0,I}$ should be provided such that the synthesized controller is guaranteed to be stable.

4. DYNAMICAL CABLE NET SYSTEM MODEL

In this section, we will first give an intuitive approach to the form control based on the inverse linearized static mapping $R(u)$. Then, we derive a dynamical system model which allows us to use robust control approaches for the controller synthesis.

4.1 Linearized Static Model and Inverse Model Control

For simplicity, let us assume that the dimensions of r and u are equal. In Section 4.3, we will justify that this assumption can be made w.l.o.g. Starting from the static equilibrium definition in Section 3, an intuitive idea to control the system is to invert

the model. As the nonlinear mapping $r = R(u)$ in (11) is not explicitly known, we linearize it around the current point $(\bar{r}, \bar{u})$. This gives us the following linearized static model

$$\Delta r = \nabla_u R(\bar{u}) \Delta u, \tag{14}$$

with
$$\nabla_u R(\bar{u}) = \nabla_r h(\bar{r}, \bar{u})^{-1} \nabla_u h(\bar{r}, \bar{u}), \tag{15}$$

because of the explicit function theorem applied to $h(\bar{r}, \bar{u}) = 0$ in (12). We refer to (Stürz et al., 2019) for more details about the derivation of (15). Note that we have passed from the absolute values of r and u to deviations Δr and Δu around the current point $(\bar{r}, \bar{u})$. Considering the linearized static model in (14), an intuitive control approach is to invert this model, i.e., to apply the control input

$$\Delta u = K_0 (r - r^{(\mathrm{des})}), \tag{16}$$

with
$$K_0 = \left(\nabla_u R(\bar{u})\right)^{-1}. \tag{17}$$

In the following, we will derive different controllers and compare them to K_0 in (17).

4.2 Dynamical Model of the Cable Net System

In the case of model uncertainties and disturbances, the control approach in (17) does not provide robust stability or performance guarantees. Therefore, we derive a discrete-time LTI dynamical system model, where the dynamics are introduced by the discrete control input steps. Let us define the state at time step k, denoted by x^k, as the deviation of the form at time step k from the desired form, i.e., $x^k := (r^{(\mathrm{des})} - r^k) \in \mathbb{R}^{n_x}$, with $n_x = 3n_I$, where r^k denotes the absolute nodal position, and the subscript k denotes the time step k. The control input to the system is denoted as $u^k := \Delta u^k \in \mathbb{R}^{n_u}$, with $n_u = m_B$, and the performance output as $e^k \in \mathbb{R}^{n_e}$. The measured output of the system, which is the input to the controller, is denoted by $y^k \in \mathbb{R}^{n_y}$. With these definitions, we consider the following dynamical system of the cable net

$$G = \begin{cases} x^{k+1} &= Ax^k + B_u u^k + B_w w^k, \\ y^k &= C_y x^k + D_{yu} u^k + D_{yw} w^k, \\ e^k &= C_e x^k + D_{eu} u^k + D_{ew} w^k, \end{cases} \tag{18}$$

where the matrices A, B_u, C_y, C_e will have the following fixed values in the remainder of the paper

$$A = I, \quad B_u = \nabla_u R(\bar{u}), \quad C_y = I, \quad C_e = I. \tag{19}$$

The other state space matrices in (18) will depend on the control problem considered and will be discussed in Section 5. In the following, we will denote by $T_{ew}(K)$ the transfer matrix from the exogenous input w^k to the performance output e^k obtained by closing the open-loop (18) with the control loop $u^k = K(y^k)$, where K denotes a discrete-time LTI controller.

First, we notice that the control approach of inverting the static mapping in (14) resulting in K_0 in (17) is a deadbeat controller for the system (18). The eigenvalues of the closed loop, i.e., of the system (18) under the controller K_0 in (17) are given by

$$\mathrm{eig}(A - B_u K_0) = \mathrm{eig}(I - \nabla_u R(\bar{u}) (\nabla_u R(\bar{u}))^{-1}) = 0. \tag{20}$$

The controller K_0 thus moves all closed loop eigenvalues of system (18) to 0, making the system converge to $x^k = 0$ in one step, which corresponds to the form r^k reaching $r^{(\mathrm{des})}$.

4.3 Controllability of the Dynamical System

So far, we made the assumption that the dimensions of the states r and the inputs u are equal, which is however only fulfilled in special cases. In general, the number of boundary edges, m_B, is smaller than the number of interior nodal coordinates, $3n_I$, and therefore $n_u < n_x$ in general. For the dynamical system G in (18), it is easy to verify that it can be controllable only if $n_u \geq n_x$. This can be seen e.g. from Kalman's rank criterion on the controllability matrix, which reveals that B_u needs to be of full row rank, which requires $n_u \geq n_x$. Therefore, the system G in (18) is uncontrollable if $m_B < 3n_I$. The system G can however always be transformed into a minimal realization for controller synthesis. Applying the synthesized controller on the system minimizes the deviations of the controllable modes in the system. In a systematic approach, a minimal realization of the system G in (18) can be computed by transforming G into its Kalman decomposition and then cutting off the uncontrollable modes. We will denote this system in the following by $G_{\min}$. This approach can always be taken, without expert knowledge of the system. It might be the case that expert knowledge about the system and the importance of individual nodal coordinates to be controlled is available. If the coordinates to be measured, i.e., C_y, can be chosen by the practitioner, then different reduced systems that are controllable and observable might be chosen depending on the choice of C_y (and the degree of controllability of the states of G). In this case, it needs to be verified that the chosen reduced system is indeed controllable (and observable). In Section 6, we will give a numerical example and demonstrate both of the proposed approaches. In the following, we assume w.l.o.g. that the system in (18) represents a minimal realization and is thus controllable.

5. ROBUST CONTROL DESIGN FOR THE NET

In this section the robust control techniques from Section 2 are applied to control the cable net in off-nominal conditions. The case of exogenous disturbances is addressed using $\mathcal{H}_\infty$ control. Then, additional model uncertainties are considered and the μ synthesis framework is leveraged.

5.1 $\mathcal{H}_\infty$ Control For Exogenous Disturbances

The starting point for the synthesis is the dynamical system formulation illustrated in Section 4. While some of the state-space matrices in (19) have fixed values given by the nature of the problem, others depend on the control task considered. The selection of these system matrices will define the closed-loop transfer matrix from w to e which we will denote by $T_{ew}(K_\infty)$. This has the same meaning as the LFT of a closed-loop transfer matrix $\mathcal{F}_l(M, K_\infty)$ used to define the optimization problem in (4). Two examples for T_{ew} are discussed next.

In the first case, we consider: $D_{yu} = D_{yw} = D_{eu} = D_{ew} = 0$. The reason is that the actuation on the cable net boundary edges involve manual measurement and adjustment steps of the edge lengths. Therefore, an uncertainty concerning the unstressed lengths of the boundary edges $l_{0,B}$ should be accounted for in the design. By recalling (10), this can be formulated as an uncertainty in the input provided to the plant. This prompts the definition of the input disturbance matrix as $B_w = \epsilon B_u$, where ϵ is a positive scalar smaller than 1 modeling the actuation uncertainty. The performance output e, depends only on the states r of the system, therefore defining a regulation problem. The associated controller and closed loop transfer matrix are denoted by $K_{\infty,1}$ and $T^r_{ew}(K_{\infty,1})$, respectively.

In the second case, we consider $D_{yw} \neq 0$, $D_{eu} \neq 0$, $D_{ew} \neq 0$ (while $D_{yu} = 0$ for physical reasons, and $B_w = \epsilon B_u$ as before). In addition to the input uncertainty as explained before,

this approach is able to capture additional exogenous disturbances, Possible disturbances can arise from external forces on the cable net in form of unmodeled forces or weights on the structure. The performance objective is now directly affected by both the exogenous disturbance and the controller (through the feedthrough matrices), and measurement noise is considered. In contrast to the previous design, the control problem now consists of both a regulation and disturbance rejection problem. The associated closed loop transfer matrix and controller will be denoted by $K_{\infty,2}$ and $T_{ew}^{d}(K_{\infty,2})$, respectively.

5.2 μ Synthesis for Modeling Uncertainty

While the previous controllers can handle exogenous disturbances, they cannot account for modeling uncertainties. However, it is known that the unstressed lengths of the interior edges $l_{0,I}$, which are subject to high fabrication variations, have a large effect on the final shape of the cable net. While in the previous section the effect of perturbations in $l_{0,B}$ was modeled as input uncertainty, perturbations in $l_{0,I}$ are inherently modeling uncertainties. In order to tackle the effect of the latter, μ controllers are proposed in the following.

We will denote the vector of nominal unstressed lengths of the interior edges by $\hat{l}_{0,I}$ in (8). The corresponding vector of uncertainties, normalized such that they can vary between -1 and +1, is denoted by $\Delta l_{0,I}$. The vector of true unstressed lengths of the interior edges are expressed as

$$l_{0,I} = \hat{l}_{0,I}(1 + \lambda_I \Delta l_{0,I}) \tag{21}$$

where λ_I is a scaling vector used to normalize the uncertainty. When an edge in the interior is considered uncertainty-free, then the corresponding entry in λ_I is set to zero.

First, an LFT model of the uncertain system is built. Given the multiplicative uncertainty in (21), this can be done by substituting (21) inside the analytic expression of $\nabla_u R$ in (15). By further substituting the uncertain operator $\nabla_u R(\Delta l_{0,I})$ in the system representation in (18), the LFT $\mathcal{F}_u(M, \Delta_l)$, where Δ_l is the structured uncertainty associated with the real uncertainties $\Delta l_{0,I}$, is obtained. This operation is performed with the RCT, followed by an LFT order reduction performed with the GSS toolbox (Biannic and Roos, 2016) to reduce the number of repetitions in Δ_l.

The final result is the uncertain closed loop transfer function $\mathcal{F}_u(\mathcal{F}_l(M, K_\mu), \Delta_l)$ (or equivalently $\mathcal{F}_u(T_{ew}(K_\mu), \Delta_l)$), which can be used in the μ synthesis problem in (6). The discussion on the different performance objectives for K_∞ in Section 5.1 carry over to K_μ.

While providing a thorough discussion on the design choices for an effective μ synthesis goes beyond the scope of the paper, a few important remarks are made here. While a standard $\mathcal{H}_\infty$ design will provide a controller K_∞ with the same number of states of the open-loop plant, the D-K iteration can lead to a controller K_μ of higher dimension due to the additional states coming from the so-called D and G scalings. These can be thought of as frequency-domain filters related to the shape of the μ plot obtained in the D step (Packard et al., 1993). In addition to the usual practice of fixing the order of the fit (which may lead to poor results because robustness of the plant is not well captured), a strategy to limit the order of K_μ is to narrow down the set of frequencies used in the D step based on an a priori knowledge of the frequency range where robustness is lacking (e.g. obtained by applying μ analysis to $\mathcal{F}_u(M, \Delta_l)$).

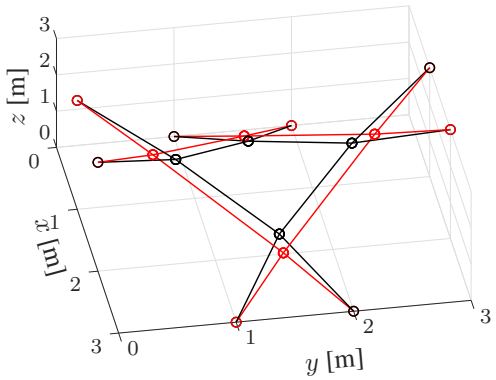

Fig. 3. Desired form, $r^{(\mathrm{des})}$ of the example cable net system (black) and initial form r^k at $k = 0$ (red).

Another strategy to reduce the order of the controllers is to apply model order reduction to K_μ. Due to the non-convexity of the D-K iteration, the initialization used for K_μ is also important. A possible choice of initialization is the controller K_∞ designed for the corresponding transfer matrix T_{ew}.

6. NUMERICAL EXPERIMENTS

In this section, we illustrate the modeling and control concepts with numerical experiments.

6.1 Example Cable Net System

We present a notional cable net system for illustrative purposes of the proposed methods and to demonstrate the effectiveness of the developed control design approaches. We consider the cable net system depicted in Fig. 3, which represents a doubly curved surface. The net consists of $n = 12$ nodes, whereof $n_I = 4$ interior nodes and $n_B = 8$ boundary nodes. The states of the overall system are given by $x = [x_1\,,\ \dots\,,\ x_4\,,\ y_1\,,\ \dots\,,\ y_4\,,\ z_1\,,\ \dots\,,\ z_4]^\top$ with dimension $n_x = 3n_I = 12$. The dimension of inputs u is $n_u = m_B = 8$, and the cable net system is not controllable. In applications involving larger scale models, model order reduction methods can be employed to reduce the number of states. However, since the controller synthesis is done offline, the computation time, and thus the dimension of the system might not be critical. In order to compute the desired form of the cable net, $r^{(\mathrm{des})}$, the boundary locations, and a uniform force density distribution for the cable net edges, are chosen. W.l.o.g. the external loads p in (13) are set to $p = 0$, i.e., we consider the cable net without the concrete, and we neglect self-weight. The material parameters EA are, w.l.o.g., assumed to be $EA = 1$ for all edges. Furthermore, p and EA are assumed to be constant. In applications where this does not hold, additional uncertainties can be introduced into the problem, analogously to the uncertainties $\Delta l_{0,I}$. In an initial design problem, the parameters of the cable net in static equilibrium are computed. The unstressed and actual edge lengths are given by $l_0 = [1_{1,4} \otimes 1.4472\,\mathrm{m},\ \ 1_{1,8} \otimes 1.3373\,\mathrm{m}]^\top$ and $l = [1_{1,4} \otimes 1.4577\,\mathrm{m},\ \ 1_{1,8} \otimes 1.3463\,\mathrm{m}]^\top$. The initial and desired coordinates are $x_0 = [1.5, 2.25, 1.5, 0.75, 1, 2, 3, 3, 2, 1, 0, 0]^\top$, $y_0 = [0.75, 1.5, 2.25, 1.5, 0, 0, 1, 2, 3, 3, 2, 1]^\top$, $z_0 = [2,\ 1,\ 2,\ 1,\ 3,\ 3,\ 0,\ 0,\ 3,\ 3,\ 0,\ 0]^\top$, and $x^{\mathrm{des}} = [1.5,\ 2.444,\ 1.5,\ 0.556,\ 1,\ 2,\ 3,\ 3,\ 2,\ 1,\ 0,\ 0]^\top$, $y^{\mathrm{des}} = [0.556,\ 1.5,\ 2.444,\ 1.5,\ 0,\ 0,\ 1,\ 2,\ 3,\ 3,$

2, 1]$^\top$, z^{des}=[2.1887, 0.8113, 2.1887, 0.8113, 3, 3, 0, 0, 3, 3, 0, 0]$^\top$. The state space matrices are then given according to (19). B_u can be computed with (15), where

$$\begin{aligned}\nabla_u h &= \left(I_3 \otimes -M_I^\top\right) \begin{bmatrix}\text{diag}(Mx_0)\\ \text{diag}(My_0)\\ \text{diag}(Mz_0)\end{bmatrix} \left(I_m \otimes \frac{EA}{2}\right) \text{diag}(l_0)^{-1} M_B,\\ \nabla_r h &= \left(I_3 \otimes -M_I^\top\right) \begin{bmatrix}\text{diag}(Mx_0)\\ \text{diag}(My_0)\\ \text{diag}(Mz_0)\end{bmatrix} \left(I_m \otimes \frac{EA}{2}\right) \text{diag}(l^{-3}) \times\\ &\quad [\text{diag}(Mx_0)\ \ \text{diag}(My_0)\ \ \text{diag}(Mz_0)]\,(I_3 \otimes M_I) \times\\ &\quad + \left(I_3 \otimes -M_I^\top\right) \left(I_3 \otimes \left(I_m \otimes \frac{EA}{2}\right)\right) \times\\ &\quad \left(I_3 \otimes \text{diag}\left(l_0^{-1} - l^{-1}\right)\right)(I_3 \otimes M_I)\,,\end{aligned} \tag{22}$$

with the incidence matrix of $\mathcal{G}$ given by $M = [M_I,\ M_B]$, with $M_I = \begin{bmatrix}\begin{bmatrix}-1 & 0 & 0 & 1\\ 1 & -1 & 0 & 0\\ 0 & 1 & -1 & 0\\ 0 & 0 & 1 & -1\end{bmatrix},\ I_4 \otimes [1,\ 1]\end{bmatrix}^\top$ and $M_B = [0_{8,4},\ -I_8]^\top$.

For a fixed input vector u, the equilibrium equations in (13) can be reformulated into an energy minimization problem which can be solved by convex programming. We refer to (Stürz et al., 2016a) for details.

6.2 Minimal Realization of the Cable Net System

In a first step, we focus on the nominal system without disturbances and illustrate the two methods to obtain a minimal realization of the system model, as proposed in Section 4.3. In both cases, the system has $q = 8$ controllable and $n_x - q = 4$ uncontrollable modes. Following the systematic approach of computing a Kalman decomposition and truncation, we obtain a minimal realization of the system, denoted by G_{min} in the following. For the second approach, we assume that the precision of the x- and y-coordinates of the interior nodes is more important than the one of the z-coordinates. We thus choose $C_y = [I_{2n_I}\ 0_{n_I}]$ and truncate the z coordinates from the system state. The resulting system, denoted by G_{xy}, is controllable. If we assume that we can only measure x and y coordinates, i.e., $C_y = [I_{2n_I}\ 0_{n_I}]$ to compute G_{min}, then G_{min} and G_{xy} are equivalent, i.e., can be transformed into each other by a regular transformation. If instead of reducing the system to x- and y-coordinates, one reduced it to y- and z-, or similarly to x- and z- coordinates, (with according choices of C_y), then uncontrollable modes would still be present in the reduced system.

6.3 Robust Control Performance

In this section the controller synthesis approaches discussed in Section 5 are applied to the proposed example cable net system where only the x- and y-coordinates are considered, i.e., the minimal realization G_{xy}.

$\mathcal{H}_\infty$ Control. The first result is that $K_{\infty,1}$ is identical to K_0. While an $\mathcal{H}_\infty$ controller has a dynamic part with a number of controller states n_{x_K} equal to the number of open-loop states, the controller matrices $A_{K\infty,1}$, $B_{K\infty,1}$, and $C_{K\infty,1}$ are zero while $D_{K\infty,1} = K_0$. Recalling that T^r_{ew} defines a regulation problem, it is expected that $K\infty, 1$ behaves like the dead-beat controller K_0.

The second $\mathcal{H}_\infty$ controller is designed considering the transfer matrix T^d_{ew} (with $D_{yw} = 0.1I_8$, $D_{eu} = 0.5I_8$, $D_{ew} = 0.5I_8$, $\epsilon = 0.2$). These values can be thought of as constant weights for the generally frequency-dependent weights used in $\mathcal{H}_\infty$ control (Balas et al., 1998). They are chosen w.l.o.g. In this case, $K_{\infty,2}$ is a dynamic LTI controller achieving the performance $\|T^d_{ew}(K_{\infty,2})\|_\infty = 0.5$, while $\|T^d_{ew}(K_0)\|_\infty = 1.2$. Fig. 4 provides a more general comparison between $K_{\infty,1}$ and $K_{\infty,2}$ by showing the singular values of $T^d_{ew}(K_0)$ (black-dashed lines) and $T^d_{ew}(K_{\infty,2})$ (blue-solid lines) over the frequency ω.

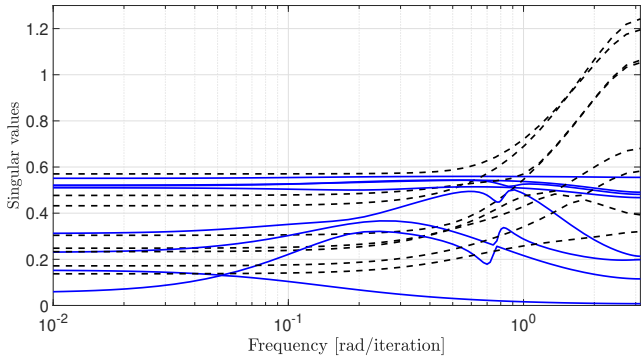

Fig. 4. Comparison of the singular values of the closed loop plants with K_0 (black-dashed) and $K_{\infty,2}$ (blue-solid).

The peaks of the two families of lines are respectively 1.2 and 0.5, but the greater robustness of $T^d_{ew}(K_{\infty,2})$ compared to $T^d_{ew}(K_0)$ can be inferred as disturbances are better rejected at all frequencies. In particular, Fig. 4 shows a lack of robustness in the K_0 closed-loop in the high frequency range (just before the Nyquist frequency π).

This first set of results shows on the one hand that the dynamical system formulation of the problem is a promising strategy to frame the robust control design of the cable net, since an $\mathcal{H}_\infty$ controller with only regulation requirements, which builds on this modeling formulation, retrieves the same *intuitive* controller K_0 designed in (17). On the other hand, when the performance objectives are different and, e.g., include disturbance rejection, $\mathcal{H}_\infty$ provides a more flexible framework to formulate the requirements and allows for greater robustness than K_0.

μ Synthesis. In the following, all interior edges are subject to an uncertainty of $\pm$ 10 % from their nominal values. Due to space constraints, and in order to provide an easy interpretation of the outcome, only the regulation problem (where T^r_{ew} is now subject to uncertainties in Δ_l) is examined. The robust controller K_μ was designed without enforcing any restriction on the order of D and G. In the D step, the frequency grid consisted of the points $[10^{-6}, 10^{-4}, 10^{-2}, 0.5, \pi]$rad/s. The order of the controller is 72, a multiple of the plant's order 8 because of the states of the scalings. Balanced truncation (Moore, 1981) is applied in order to obtain $n_{x_K} = 8$ states, and the associated controller is denoted by $K_{\mu,r}$. Fig. 5 shows a comparison of the RP test for the controllers by showing the upper bound of μ_Δ. It is confirmed that the dead-beat controller K_0 shows a poor performance in the high frequency range and it has a μ peak of 10.8, while the peak for $K_{\mu,r}$ is 9.1. That is, a guaranteed 20 % increase of robust performance is achieved. Generally, μ analysis carries important frequency information which can be used to speculate on the causes for the lack of robustness (Iannelli et al., 2018). E.g., inspection of the worst-case combination of the uncertain parameters can point out modeling aspects which deserve particular care in order to increase robustness. In addition, the peak frequency of a μ stability plot is associated with the eigenvalue responsible for the neutral stability of the

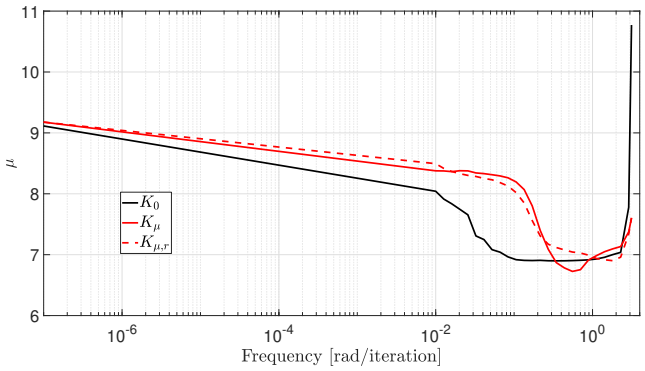

Fig. 5. Comparison of μ (upper bound) for different closed loop plants.

system. In the case of discrete time systems, the frequency of the peak thus corresponds to the phase of the pole(s) lying on the unit disk when subject to the worst-case perturbation.
Both μ controllers are able to decrease the maximum peak of the plot and thus the plant's robustness to the uncertainty. Moreover, robust performance is not substantially affected when the reduced order controller is tested. A comparison of the RS test revealed very similar plots to those in Fig. 5. This is not surprising since for the regulator problem the worst-case combination of the uncertainties for performance is the same as for stability. I.e., the loss of robustness in performance is due to the plant becoming unstable due to the uncertainty. That is, the cable net does not converge to the desired shape and the discrete application of control inputs leads to a diverging response.

By definition, if the peak of μ is larger than 1, the system does not achieve robust performance. Hence, Fig. 5 shows that for variations of unstressed lengths within $\pm$ 10 %, none of the controllers guarantee RP. This is not surprising since this is a large range for real applications. To better quantify the improvements by the robust control solutions, 4 different uncertainty ranges were considered, namely 1 %, 2 %, 3 %, 5 % and 10 %. For each range, 1000 realizations of the uncertainty were uniformly sampled and system (18) was simulated under K_0 and $K_{\mu,r}$. This test was performed 10 times, and the average number of failures in convergence of the control iteration in (18) is reported in Table 1.

Table 1. Percentage of failures (over 1000 tests).

Uncertainty range	1 %	2 %	3 %	5 %	10 %
K_0	0*	23.2	42.8	53.4	66.4
$K_{\mu,r}$	0	7.7	10.1	10.7	17.4

While according to the worst-case RP test in Fig. 5 the increase of robustness achieved by $K_{\mu,r}$ is of the order of $\frac{10.8}{9.1} \cong 1.2$, simulations show that for randomly generated perturbations the increase of robustness with the μ controller is much higher. It goes from $\frac{23.2}{7.7} \cong 3$ for the case of 2 % to $\frac{53.4}{10.7} \cong 5$ for the case of 5 %. The reason for the $*$ for K_0 in the case of 1 % range is that since the peak of curve K_0 in Fig. 5 is greater than 10, there exists a worst-case perturbation which makes the iteration diverge. This perturbation was extracted from the lower bound calculation of μ and its effect confirmed in simulation. It was however not found in the Monte Carlo campaign, and shows the power of robust control techniques in detecting analytically worst-case perturbations for uncertain systems. On the other hand, the peak of the curve $K_{\mu,r}$ is below 10 and thus the associated system is guaranteed to be stable for any perturbation in that range.

7. CONCLUSION

A novel modeling approach of prestressed cable net systems as discrete-time LTI systems was presented together with the synthesis of robust controllers. $\mathcal{H}_\infty$ control was used to take into account input uncertainties and external disturbances, while μ synthesis was adopted to take into account additional parametric uncertainties. A numerical case study illustrated that both control designs outperform analytically (maximum singular value and μ analysis plots) and in simulation a deadbeat controller designed by inverting the model.

REFERENCES

Balas, G., Doyle, J., Glover, K., Packard, A., and Smith, R. (1998). *μ Analysis and Synthesis Toolbox*.

Biannic, J.M. and Roos, C. (2016). Generalized State Space: a new Matlab class to model uncertain and nonlinear systems as Linear Fractional Representations, available at http://w3.onera.fr/smac//gss.

Doyle, J. and Stein, G. (1981). Multivariable feedback design: Concepts for a classical/modern synthesis. *IEEE Transactions on Automatic Control*, 26(1), 4–16.

Iannelli, A., Marcos, A., and Lowenberg, M. (2018). Study of Flexible Aircraft Body Freedom Flutter with Robustness Tools. *J. Guid. Control Dynam.*, 41(5), 1083–1094.

Liew, A., Stürz, Y.R., Guillaume, S., Van Mele, T., Smith, R.S., and Block, P. (2018). Active control of a rod-net formwork system prototype. *Autom. Constr.*, 96, 128–140.

Lydon, G.P., Hofer, J., Svetozarevic, B., Nagy, Z., and Schlueter, A. (2017). Coupling energy systems with lightweight structures for a net plus energy building. *Appl. Energy*, 189(2017), 310–326.

Moore, B.C. (1981). Principal Component Analysis in Linear Systems: Controllability, Observability, and Model Reduction. *IEEE Trans. Automat. Contr.*, 26(1), 17–32.

Packard, A. and Doyle, J. (1993). The Complex Structured Singular Value. *Automatica*, 29(1), 71–109.

Packard, A., Doyle, J., and Balas, G. (1993). Linear, multivariable robust control with a μ perspective. *Journal of Dynamic Systems, Measurement, and Control*, 115(2B), 426–438.

Stürz, Y.R. (2019). Optimization-based and distributed control for digital fabrication. *Ph.D. Thesis, ETH Zurich, Switzerland*.

Stürz, Y.R., Khosravi, M., and Smith, R.S. (2020). Parameter identification for digital fabrication: A Gaussian process learning approach. *IFAC Papers Online*. [to appear].

Stürz, Y.R., Morari, M., and Smith, R.S. (2019). Control of an Architectural Cable Net Geometry. *IEEE Trans. Control Syst. Technol.* doi:10.1109/tcst.2019.2910449.

Stürz, Y.R., Morari, M., and Smith, R.S. (2016a). Sequential quadratic programming for the control of an architectural cable net geometry. *Am. Control Conf.*, 3503–3508.

Stürz, Y.R., Morari, M., and Smith, R.S. (2016b). Two methods for the identification of uncertain parameters of an architectural cable net geometry. *IEEE Conf. Control Appl.*, 804–809.

Torsing, R., Bakker, J., Jansma, R., and Veenendaal, D. (2012). Large-scale designs for mixed fabric and cable net formed structures. *Int. Conf. Flex. formwork*, 346–355.

Veenendaal, D., Bezbradica, M., Novák, D., and Block, P. (2014). Controlling the geometry and forces of a hybrid cable-net and fabric formwork for thin concrete shells. *IASS-SLTE Symp.*, 170–177.

Zhou, K., Doyle, J.C., and Glover, K. (1996). *Robust and Optimal Control*. Prentice-Hall, Inc.